Int. J. Solids Structures, Vol. 11, pp. 377–401. Pergamon Press 1975. Printed in Great Britain

A FINITE ELEMENT ANALYSIS OF SHOCKS AND FINITE-AMPLITUDE WAVES IN ONE-DIMENSIONAL HYPERELASTIC BODIES AT FINITE STRAIN

R. B. FOST

Teledyne Brown Engineering Co., Huntsville, Alabama, U.S.A.

and

J. T. ODEN and L. C. WELLFORD, JR.

Texas Institute of Computational Mechanics, Univ. of Texas, Austin 78712, U.S.A.

(*Received* 18 *October* 1972; *revised* 25 *March* 1974)

Abstract—The general theory of shock and acceleration waves in isotropic, incompressible, hyperelastic solids is used in conjunction with the concept of finite elements to construct discrete models of highly nonlinear wave phenomena in elastic rods. A numerical integration scheme which combines features of finite elements and the Lax–Wendroff method is introduced. Numerical calculations of the critical time for shock formulation are given. Numerical results obtained from representative cases are discussed.

1. INTRODUCTION

Until very recent times, the quantitative study of the dynamic response of highly elastic solids at finite strain has stood outside the reach of existing analytical and computational methods. The complete dynamical theory, is, itself, still being pieced together some 20 years after the modern era of finite elasticity began (e.g. [1, 2]), and while a few solutions to finite-amplitude vibration problems have been contributed (e.g. [3–5] or, for additional references, [6]), and while some advances have been made in the theory of finite elastic waves (e.g. [7–9]), actual calculations invariably involve rather ideal geometries, boundary and initial conditions, and/or material properties. The highly nonlinear character of the momentum equations for the most simple hyperelastic material does not account for all of the computational problems—by definition, the hyperelastic solid possesses no dissipative mechanism to provide smoothing or damping of higher frequencies. Consequently, the computationally convenient features of damping encountered in nonlinear viscoelasticity and thermoviscoelasticity calculations [10–12] are not present. To complicate matters, it is now generally recognized that shock waves can be easily produced in such materials, even when smooth initial conditions are prescribed. The recent experimental work of Kolsky [13] gives evidence to the possibility of even tensile shock waves developing in certain stretched natural rubbers, a phenomena already anticipated in the theoretical work of Bland [8] and Chu [9]. In such cases, practically all of the popular numerical integration schemes now used in structural dynamics are ineffective.

In the present paper, we consider an important subclass of the problems alluded to in our opening comments, and we demonstrate that the finite-element method, when used in conjunction with established methods of computational hydrodynamics and implemented with

modern computing machinery, can be extremely effective for this class of problems. More specifically, the present paper is concerned with the application of the finite-element method to the calculation of shock waves and finite-amplitude acceleration waves in highly elastic rubber-like materials. So as not to obscure conceptual and physical details, this investigation is confined to the study of only longitudinal motions of finite homogeneous rods of isotropic, incompressible, hyperelastic materials. We hope to treat the more difficult problems of finite-amplitude waves in two- and three-dimensional hyperelastic bodies in later work. Herein, we develop a fully discrete representation of the behavior which employs a finite-element approximation of the spatial variation of the displacement field or the longitudinal extension ratio and a finite-difference representation of the temporal behavior. For shock calculations, we introduce an apparently new explicit integration scheme which is shown to be very effective in handling the formation, propagation, and reflection of shocks in disturbed media. The scheme involves the use of finite-elements as a basis for formulating Lax–Wendroff-type time integration algorithms. Moreover, we also consider the problem of computing numerically various critical times required for the formation of shocks from smooth and Lipschitz-continuous initial data. In the final section of the paper, we cite numerical results obtained from a number of representative test cases.

2. PHYSICS OF WAVES IN NONLINEAR ELASTC MATERIALS

In this section, we shall review certain features of the dynamical and thermodynamical theory of finite elasticity that are essential to our study. More complete details can be found in the books of Green and Zerna[14], Green and Adkins[15], and Bland[8], and certain special features are discussed in the papers of Nowinski[16], Ames[17], and Reddy and Achenbach[18].

2.1 *Motion of a thin rod*

We begin by considering longitudinal motions of a thin rod of isotropic, incompressible material. While at rest in a natural reference configuration $\mathscr{R}_0$, the rod has a uniform symmetric cross section of area A_0, a length L_0, and a mass density ρ_0. To describe the motion of the rod relative to its reference configuration, we establish a fixed spatial frame of reference x, with origin o at one end of the bar, which is assumed to be restrained from motion. We denote by X the labels of material particles (material coordinates) of the bar, and we select these labels so as to numerically coincide with the spatial coordinates x when the bar occupies its reference configuration. The function $x = x(X, t)$ then gives the spatial position of the particle X at time t and defines the longitudinal motion of the bar, while $u(X, t) \equiv x(X, t) - X$ defines the displacemjent of particle X at time t.

The material gradient $\partial x/\partial Y$ serves as a convenient measure of the deformation; physically, it represents the longitudinal extension ratio λ (also called the stretch) which is expressible in terms of the displacement gradient according to

$$\lambda = \frac{\partial x}{\partial X} = 1 + \frac{\partial u}{\partial X} = 1 + u_x \tag{2.1}$$

where here, and henceforth, we use the subscript notation $u_x = \partial u/\partial X$ to denote partial differentiation with respect to X. The extensional strain γ is then simply $(\lambda^2 - 1)/2$.

Now any disturbance supplied to the rod will travel with finite speed from one particle to another in the form of a surface (curve) of discontinuity S (a wave) in the X–t plane. If we denote by $Y(t)$ the particle X reached by a wave front at time t, then the set of points $(Y(\tau), \tau), \tau$

being a real parameter, defines a curve in the X–t plane across which jump discontinuities in various partial derivatives of $u(X, t)$ can occur. Indeed, acceleration waves involve jumps in the acceleration u_{tt} (and the stress gradient $\partial\sigma/\partial X$) and shock waves (shocks) involve the propagation of surfaces across which jump discontinuities in the velocity $\dot{u}(X, t) = u_t = \partial u/\partial t$ and the stress are experienced. The intrinsic wave speed relative to the material, denoted c, is then simply $\mathrm{d}Y(t)/\mathrm{d}t$. However, the *spatial* position $y(t)$ of the wave is clearly

$$y(t) = x(Y(t), t) \tag{2.2}$$

and the absolute wave speed, as seen by a stationary observer, is

$$v = \frac{\mathrm{d}y(t)}{\mathrm{d}t} = \frac{\mathrm{d}x(Y(t), t)}{\mathrm{d}t}. \tag{2.3}$$

2.2 *The balance laws*

We assume, of course, that the response of the bar satisfies the basic conservation laws of physics. For the problem at hand, these assume the following global forms:

Linear momentum

$$A_0 \int_{L_0 - Y(t)} (\rho_0 \ddot{u} - \sigma_x)\, \mathrm{d}x + A_0 [\![\sigma + \rho_0 \dot{u} c]\!]_Y = 0. \tag{2.4}$$

Energy

$$A_0 \int_{L_0 - Y(t)} (\rho_0 \dot{u}\ddot{u} + e - \sigma_x \dot{u} - \sigma \dot{u}_x - q_x)\, \mathrm{d}x + A_0 \left[\!\!\left[\frac{1}{2} \rho_0 c \dot{u}^2 + ce + \sigma \dot{u} + q \right]\!\!\right]_Y = 0. \tag{2.5}$$

Calsius Duhem-inequality

$$A_0 \int_{L_0 - Y(t)} \left[\xi - \left(\frac{q}{\theta} \right)_x \right] \mathrm{d}x + A_0 \left[\!\!\left[c\xi + \frac{q}{\theta} \right]\!\!\right]_Y \geq 0. \tag{2.6}$$

Here $\sigma(X, t)$ is the first Piola–Kirchhoff stress, e is the internal energy per unit initial volume, q is the heat flux, ξ is the entropy per unit initial volume, and θ is the absolute temperature. Quantities in brackets denote jumps suffered at the surface of discontinuity $(Y(t), t)$; e.g.

$$[\![\sigma]\!]_Y = \sigma(Y(t^-), t) - \sigma(Y(t^+), t), \tag{2.7}$$

etc. Mass is conserved in the rod and we have ignored body forces and internal heat sources for simplicity.

At particles X that do not fall on a surface of discontinuity, (2.4)–(2.6) lead to the local forms of the balance laws

$$\begin{aligned} \rho_0 \ddot{u} - \sigma_x &= 0 \\ \dot{e} - \sigma \dot{\lambda} - q_x &= 0 \\ \theta \dot{\xi} - q_x + \frac{q\theta_x}{\theta} &\geq 0. \end{aligned} \tag{2.8}$$

Whereas at the surface of discontinuity, we obtain the jump conditions:

$$\begin{aligned} \rho_0 c[\![\dot{u}]\!]_Y + [\![\sigma]\!]_Y &= 0 \\ \tfrac{1}{2}\rho_0 c[\![\dot{u}^2]\!]_Y + c[\![e]\!]_Y + [\![\sigma\dot{u}]\!]_Y + [\![q]\!]_Y &= 0 \\ c[\![\xi]\!]_Y + \left[\!\left[\frac{q}{\theta}\right]\!\right]_Y &\geq 0. \end{aligned} \tag{2.9}$$

The equation $(2.9)_2$ is the energy jump condition. We now assume that $(2.9)_1$ is identically satisfied and define the average material velocity at the jump by

$$\hat{\dot{u}} = \frac{\dot{u}^+ + \dot{u}^-}{2}$$

where $\dot{u}^+ = \dot{u}(Y(t^+), t)$ and $\dot{u}^- = \dot{u}(Y(t^-), t)$. The first term in $(2.9)_2$ then takes the form

$$\begin{aligned} \frac{1}{2}\rho_0 c[\![\dot{u}^2]\!]_Y &= \frac{1}{2}\frac{[\![\sigma]\!]_Y [\![\dot{u}^2]\!]_Y}{[\![\dot{u}]\!]_Y} \\ &= -[\![\sigma]\!]_Y \hat{\dot{u}} \end{aligned} \tag{2.10}$$

introducing (2.10) into $(2.9)_2$ and setting $\Delta\dot{u} = \dot{u} - \hat{\dot{u}}$, we see that

$$c[\![e]\!]_Y + [\![\sigma\Delta\dot{u}]\!]_Y + [\![q]\!]_Y = 0. \tag{2.11}$$

Another form can be obtained by defining the average stress

$$\bar{\sigma} = \frac{\sigma^+ + \sigma^-}{2}.$$

We notice that $[\![\sigma\Delta\dot{u}]\!]_Y = \bar{\sigma}[\![\dot{u}]\!]_Y$. Thus

$$c[\![e]\!]_Y + \bar{\sigma}[\![\dot{u}]\!]_Y + [\![q]\!]_Y = 0. \tag{2.12}$$

Equation (2.12) will be called the *local jump condition for energy.*

It is often convenient to introduce the Helmholtz free energy $\phi(X, t)$ and the internal dissipation $\delta(X, t)$ defined for $X \neq Y(t)$ by

$$\phi = e - \xi\theta \quad \text{and} \quad \delta = \theta\dot{\xi} - q_x \tag{2.13}$$

then $(2.9)_3$ can be rewritten in the alternate form

$$\delta + \frac{q\theta_x}{\theta} = \sigma\dot{\lambda} - \dot{\phi} + \xi\dot{\theta} + \frac{q\theta_x}{\theta} \geq 0. \tag{2.14}$$

In addition, we can also impose Maxwell's theorem, which asserts that for any function $f(X, t)$ jointly continuous in X and t, but whose first partial derivatives f_x and $\dot{f}$ suffer jump discontinuities at S, the jump across S in the (two-dimensional) gradient of f must be parallel to a

vector $(-1, c)$ normal to S. Applying this idea to the motion $x(X, t)$ yields Hadamard's compatibility condition:

$$[\![\dot{u}]\!]_Y + c[\![\lambda]\!]_Y = 0. \tag{2.15}$$

2.3 *Waves in hyperelastic materials*

We now aim our analysis toward waves in hyperelastic materials; that is, we wish to consider materials for which there exists a potential W which is a function of the current value of λ, and for which

$$\dot{W} = \sigma\dot{\lambda} \quad \text{and} \quad \sigma = \frac{\partial W}{\partial \lambda}. \tag{2.16}$$

The question arises, however, as to whether or not a theory of hyperelasticity is reconcilable within the thermodynamic framework established thusfar. This is a classic question, and standard arguments can be found in a number of places (e.g. [6, 12]) to the effect that hyperelasticity is indeed possible in a number of physically meaningful situations. The fact that these standard arguments are not valid at surfaces of discontinuity is fundamental to the physics of shock waves.

We mention two cases. First, consider a class of perfect materials (see [6], p. 296), the constitution of which is defined by equations for e, σ, θ and q depicted as functions of the current values of λ and ξ, with q also dependent on $\theta_x(X, t)$. For reversible processes performed on such materials, the dissipation $\delta = \theta\dot{\xi} - q_x = 0$, and $(2.8)_2$ gives

$$\left(\sigma - \frac{\partial e}{\partial \lambda}\right)\dot{\lambda} + \left(\theta - \frac{\partial e}{\partial \xi}\right)\dot{\xi} + \frac{1}{\theta} q\theta_x \geq 0 \tag{2.17}$$

so long as $X \in (L_0 - Y(t))$. Secondly, we consider a class of simple materials (see [12], p. 202) whose constitution is defined by equations for φ, σ, ξ and q in terms of current values of λ and θ, with q dependent upon $\theta_x(X, t)$ also. For reversible process ($\sigma = 0$), using (2.13) in (2.8) gives us the inequality

$$\left(\sigma - \frac{\partial \varphi}{\partial \lambda}\right)\dot{\lambda} - \left(\xi + \frac{\partial \varphi}{\partial \theta}\right)\dot{\theta} + \frac{1}{\theta} q\theta_x \geq 0 \tag{2.18}$$

for all $X \in (L_0 - Y(t))$. If these two inequalities, (2.17) and (2.18), are to be maintained for arbitrary rates, it necessarily follows (see [12], p. 214) that in the absence of a shock, a theory of hyperelasticity is appropriate for reversible isentropic processes ($\delta = 0$, $\dot{\xi} = 0$) performed on the above class of perfect materials and for reversible isothermal processes ($\delta = 0$, $\dot{\theta} = 0$) performed on the above class of simple materials. In the former case, the strain energy is associated with the internal energy, in the latter case it is associated with the free energy. However, since a shock is characterized by discontinuities in the displacement gradient, the necessary derivatives of e in (2.17), or of φ in (2.18), do not exist for $X = Y(t)$. Therefore, we must have energy dissipation at $X = Y(t)$, i.e. $\delta = \theta\dot{\xi} - q_x > 0$, and we lose the notion of reversibility.

Due to the considerable difficulties involved in solving the nonlinear thermo-mechanical equations governing irreversible thermodynamic processes, the only exact solutions available [19, 20] are for shocks with uniform conditions on both sides of the discontinuity. Hence, for additional solutions, we need to simplify the governing equations so that they become

tractable. One possibility, suggested by the exact discontinuous solutions themselves, is the well known fact that "weak shocks" are nearly isentropic (e.g. see [8, 21, or 22] for detailed discussions). That is, taking the proportional change in magnitude across the shock of some state parameter, say u_x, as a measure of shock "strength", the change in entropy across the shock is only of third order in the shock strength for small changes of u_x. Therefore, for weak shocks, we can neglect the entropy change and consider ξ as constant for all X and t, i.e. the deformation takes place isentropically. It is of special interest to consider this "isentropic approximation" when the initial, or reference configuration is the natural stress-free state where $\lambda(X, 0) = 1$, $\theta(X, 0) = T_0 = \text{constant}$. Then the isentropic approximation becomes $\xi = 0$ everywhere for all time. Moreover, for this case, the isentropic approximations render the mechanical equations independent of the thermal equations, and the mechanical jump conditions (the first of (12.9) and (12.15)) alone are sufficient to determine the shock process. (Naturally the energy jump condition remains valid, but here it would only be used to check the energy balance after solving the problem.) Also, we can readily define the strain energy function W of (2.16) in terms of the internal energy $W(\lambda) = e(\lambda, \xi)|_{\xi=0}$, so that we have the constitutive relation for the stress $\sigma = \partial e/\partial\lambda$, in agreement with (2.16).

We remark that the local balance laws (2.8) suggest another simplification: the adiabatic approximation, wherein we assume the heat conduction small enough to take $q = 0$. Outside the shock region, the adiabatic process is reversible ($\delta = 0$); and then from (2.13) we get the reversible adiabatic process to be an isentropic process. Hence, in regions of the rod where $X \neq Y(t)$, a theory of hyperelasticity, in the sense of (2.17), is possible. At the shock, the adiabatic process is not reversible: entropy is produced. Then, by integrating the inequality in (2.8) with $q = 0$, we get $\xi = \xi(X)$. Therefore the entropy at each material point has a constant value unless a shock passes over the point, at which time the value of the entropy is changed to a new constant. Consequently, until the time at which a shock forms, the adiabatic process is isentropic for every $X \in (0, L_0)$; after this time, the adiabatic process is, in general, piecewise isentropic, i.e. it is isentropic for every $X \in \{(0, Y(t^-)], [Y(t^+), L_0)\}$.

Both of these assumptions can, of course, be simultaneously incorporated if we consider the propagation of weak adiabatic shocks. In this case, again following (2.17), the material will be everywhere hyperelastic at all times.

3. EVOLUTION AND PROPAGATION OF DISCONTINUITIES

In this section we will look at the physical conditions which are generally required for the formation and propagation of discontinuities—both shock waves and acceleration (simple) waves in rubber-like materials. We also briefly consider methods for determining the time required for discontinuities to evolve during the solution process.

3.1 *Propagation of shock and acceleration waves*

In the absence of shocks, we previously obtained the first member of (2.8) as the local form of the law of conservation of linear momentum. In view of the constitutive relation (2.13) for hyperelastic materials we have $\sigma = \sigma(\lambda)$, so that the local momentum equation for such materials can be written in the form

$$\ddot{u} - c^2(u_x)u_{xx} = 0 \tag{3.1}$$

where the squared intrinsic wave speed, $c^2(u_x)$, is given by

$$c^2(u_x) = \frac{1}{\rho_0}\frac{d\sigma}{d\lambda}. \tag{3.2}$$

We also note that, since $\dot{\lambda} = \dot{u}_x$, we can recast the local momentum equation (3.1) in terms of λ according to

$$\ddot{\lambda} = [c^2(\lambda)\lambda_x]_x \tag{3.3}$$

where, clearly, the forms of $c^2(\lambda)$ and $c^2(u_x)$ will be different.

As noted earlier, for hyperelastic solids the stress is derivable from a potential function W which represents the strain energy per unit undeformed (reference) volume v_0. For isotropic incompressible bodies, W is generally defined in terms of the first two principal invariants, I_1 and I_2, of Green's deformation tensor, the third principal invariant being unity. In the present case, $I_1 = 2\lambda^{-1} + \lambda^2$, $I_2 = 2\lambda + \lambda^{-2}$, and elimination of the hydrostatic pressure with the condition that transverse normal stresses are zero, leads to the general constitutive law

$$\sigma = 2(W_1\lambda + W_2)(1 - \lambda^{-3}) \tag{3.4}$$

where $W_\alpha = \partial W/\partial I_\alpha$, $\alpha = 1, 2$. Substituting (3.4) into (3.2), we observe that the square of the wave speed in materials defined by (3.4) is of the form

$$c^2 = \frac{2}{\rho_0}[(1 + 2\lambda^{-3})W_1 + 3\lambda^{-4}W_2 + 2(1 - \lambda^{-3})^2(W_{11}\lambda^2 + 2W_{12}\lambda + W_{22})]. \tag{3.5}$$

If we eliminate, on physical grounds, the possibility of complex wave speeds, we, in turn, impose conditions on the form of W and its derivatives W_α, $W_{\alpha\beta}$. In this regard, we shall assume that the stress σ is a continuous monotonically increasing function of the stretch λ, so that for all $\lambda \in (0, \infty)$, we have $0 < \rho_0 c^2(\lambda) = d\sigma/d\lambda < \infty$. This important property allows us to interpret qualitatively a number of interesting nonlinear wave phenomena. For example, suppose that a time-dependent surface traction is applied at the free end of the rod. During each infinitesimal increment in time, the corresponding increment in load produces a "wavelet," so that, using Nowinski's terminology[16], the net effect of the loading is to produce an "infinite manifold" of wavelets propagating along the rod. Obviously, each successive wavelet propagates at a speed determined by the instantaneous slope of the σ vs λ curve for the material. Thus if consecutive wavelets are propagated with decreasing speeds, the slope of the wave front will gradually decrease (contrasting markedly with the usual sharp discontinuity at the wave front in materials with linear σ–λ curves), and the response will be propagated as a simple wave. However, if the distance between successive wavelets decreases during propagation (they are generated with increasing speeds), the wave profile steepens until the discontinuity is transformed into a shock wave.

To be more specific, consider, for example, the following special forms of the strain energy function:

(i) The neo-Hookean form, $W = C(I_1 - 3)$ (3.6)

(ii) The Mooney form, $W = C_1(I_1 - 3) + C_2(I_2 - 3)$ (3.7)

(iii) The Biderman form, $W = B_1(I_1 - 3) + B_2(I_1 - 3)^2 + B_3(I_1 - 3)^3 + B_4(I_2 + 3)$. (3.8)

Here C, C_1, $C_2, \ldots, B_4$ are material constants. Examples of a variety of other forms of W proposed for real materials are summarized in [12]. Note that for Mooney materials

$$c^2 = \frac{2}{\rho_0}[C_1(1 + 2\lambda^{-3}) + 3C_2\lambda^{-4}] \tag{3.9}$$

whereas in the case of Biderman materials

$$c^2 = \frac{2}{\rho_0}\{[B_1 + 2B_2(2\lambda^{-1} + \lambda^2 - 3) + 3B_3(2\lambda^{-1} + \lambda^2 - 3)^2](1 + 2\lambda^{-3}) + 3B_4\lambda^{-4} + [4B_2 + 12B_3(2\lambda^{-1} + \lambda^2 - 3)](\lambda - \lambda^{-2})^2\}. \tag{3.10}$$

The function c^2 for neo-Hookean materials follows from (3.9) by setting $C_2 = 0$. Equations (3.6)–(3.8) with (3.4) and (3.9) and (3.10) describe σ–λ and c–λ curves of the type shown in Figs. 1 and 2. Clearly, the type of wave generated by an initial disturbance depends upon both the initial state (i.e. the initial value of λ) and whether λ is subsequently increased or decreased. A discontinuity is propagated as a simple wave if, and only if, the intrinsic wave speed of the material in front of the discontinuity is greater than that of the material behind the discontinuity

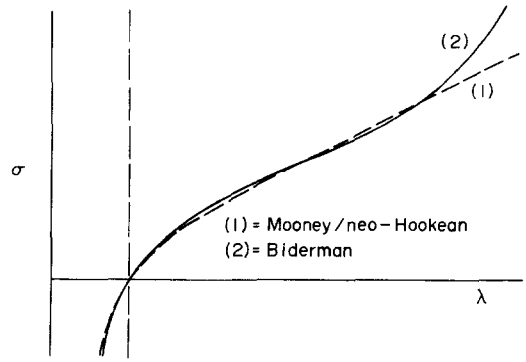

Fig. 1.

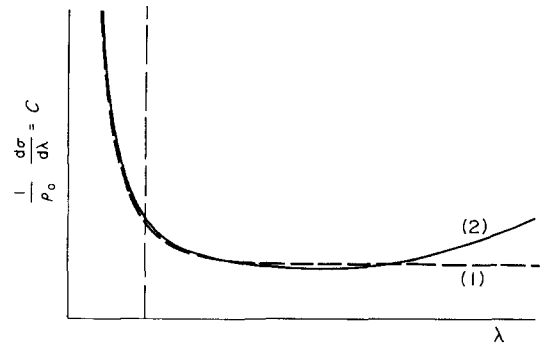

Fig. 2.

(see [21], p. 243). Hence, Fig. 2 suggests that for both the Mooney and neo-Hookean materials, only compression shock waves can be developed. However, for certain Biderman-type materials (curve (2) in Fig. 2), it is possible to produce a tensile shock wave if the material is prestretched sufficiently. The development of such tensile shocks has, in fact, been observed experimentally by Kolsky[13]. It is also interesting to consider the case in which an applied tension load is suddenly removed. From Fig. 2 we can see that this discontinuity cannot be propagated by a simple wave since the wave speed is smaller before the load is released than after. Thus, it follows that the instant the stress at the end of the rod begins to decrease (after having increased) is also the time at which the first wavelet emanates from the end with a propagation speed faster than the preceding wavelets. Therefore, at some time subsequent to the moment when the unloading starts, the propagated influence of this release, or unloading, is expected to develop into a shock wave.

3.2 *Evolution of discontinuities*

The formation of discontinuities in solutions of nonlinear hyperbolic equations has been a topic of interest for many years. The research on this topic falls into two principal categories: discontinuities which evolve from Lipschitz continuous initial data and those which evolve from smooth initial data. In the former case, there is a clearly defined wave front and a characteristic along which the initial discontinuity (even when starting with analytic initial data, a Lipschitz discontinuity can subsequently develop) propagates until it tends to a jump discontinuity at some critical time, say t_{CR}. This jump discontinuity then propagates in a completely different manner from the Lipschitz discontinuity. As this is discussed in detail in [8, 21, and 23], we will mention only the essential features.

In general, the characteristics of the nonlinear wave equation are curved lines in the X–t plane. However, if a constant initial state is prescribed for the rod, the characteristics of positive slope are a family of straight lines and the corresponding wave is a simple (acceleration) wave. If the excitation at the end of the rod is such that successive wavelets are generated with decreasing shift rates, these straight characteristics diverge in the X–t plane. But, if the shift rate at the end of the rod increases (e.g. due to compression or, sometimes, sufficient tension with an "S-shaped" σ–λ curve), the characteristics of positive slope will no longer diverge. Instead, they converge and form an "envelope" as shown in Fig. 3. It is on this envelope that the value of

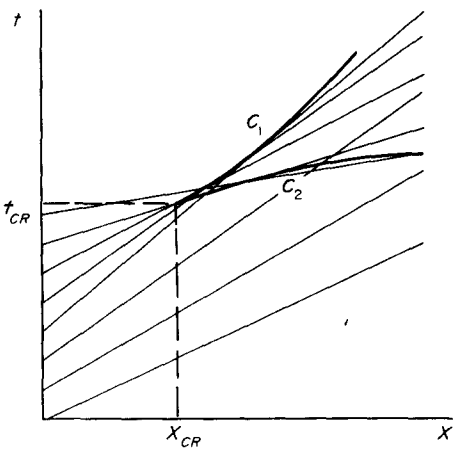

Fig. 3.

velocity and stress, carried by the characteristics, conflict so that the curve C_2 is an approximation of a shock wave propagating with variable speed and carrying a variable stress. The earliest time that such an envelope appears, i.e. when the first two characteristics converge, a cusp is formed at some point X_{CR}. At this point (X_{CR}, t_{CR}) a unique solution of the wave motion, characterized as a simple wave, is mathematically impossible. It is the jump conditions which enable us to continue past (X_{CR}, t_{CR}) with a unique solution for the shock.

The second category; the evolution of discontinuities from smooth initial data, is the topic which seems to be of current interest (see e.g. [17, 24–26]). When applicable, the method presented by Ames[17, 24] is the simplest and the most accurate. This method results from observing that classes of quasilinear equations can be obtained by differentiation of first-order nonlinear equations. The first order equations are then used to calculate the time t_{CR}.

For the one-dimensional rod considered herein, we find from [17] that the critical time is given by

$$t_{CR} = \min \frac{1}{h'\phi'} \tag{3.11}$$

where primes mean differentiation of the quantity with respect to the argument and the forms of h and ϕ depend upon which form of the wave equation we are considering, (3.1) or (3.3). For the displacement form of the equation of motion, (3.1), we have

$$u_x = h[X + c(u_x)t] \tag{3.12}$$

$$\phi = c(u_x) \tag{3.13}$$

with $c(u_x)$ being the material shift rate defined in (3.2). If we consider (3.3) on the other hand, we have

$$\lambda = h[X + \phi(\lambda)t] \tag{3.14}$$

$$\phi = c(\lambda) \tag{3.15}$$

where the form of $c(\lambda)$ is given in (3.5).

4. FINITE ELEMENT APPROXIMATIONS

We are now ready to develop discrete models of the equations governing nonlinear waves by using the finite-element concept. Toward this end, we begin, as usual, by partitioning the rod into a finite number E of segments connected together at nodal points at their ends. The $E + 1$ nodes are labeled $0 = X^1 < X^2 < \ldots < X^{E+1} = L_0$, and the mesh length $h = X^{\alpha+1} - X^\alpha$ $(\alpha = 1, 2, \ldots, E)$ is assumed to be uniform. In the finite-element method for nonlinear waves, we seek approximate solutions for the displacement field u, the solution to (3.1), or the extension ratio (stretch) λ, the solution to (3.3), in a finite dimensional subspace $S_h^1(0, L_0)$ or $S_h^2(0, L_0)$ of the original solution space $H^1(0, L_0)$. We could introduce an approximation for u of the form

$$u(X, t) = u_\alpha(t)\hat{\eta}_\alpha(X) \tag{4.1}$$

where $u_\alpha(t)$ are the nodal values of the displacement, $\hat{\eta}_\alpha(X)$ is a basis for $S_h^1(0, L_0)$, and the

repeated index α is summed from 1 to $E+1$. Similarly, we could introduce an approximation for λ of the form

$$\lambda(X,t) = \lambda_\alpha(t)\hat{\psi}_\alpha(X) \tag{4.2}$$

where $\lambda_\alpha(t)$ are the nodal values of the extension ratio and $\hat{\psi}_\alpha(X)$ is a basis for $S_h^2(0, L_0)$. In general, the functions $\hat{\eta}_\alpha(X)$ and $\hat{\psi}_\alpha(X)$ are generated from local (elemental) basis functions.

In the finite-element method, it is convenient to first describe the behavior of each element independently in terms of the nodal values; the entire set of elements is then connected together by establishing the nodal connectivity. Hence we now take advantage of this fundamental property of finite-element models and temporarily focus our attention on a typical element from the assemblage representing the continuous rod.

To construct the finite model of an elemental field quantity, say $f(X,t)$, we introduce the approximating functions for each element which are locally of the form

$$f(X,t) \doteq f_\alpha(t)\psi_\alpha(X). \tag{4.3}$$

For simplicity, we consider only first-order representations, so that the repeated index α is a nodal index which ranges from 1 to 2 for the one-dimensional rod element. Here, $f_\alpha(t)$ is the value of $f(X,t)$ at node α of the element at time t, and $\psi_\alpha(X)$ are the usual local (elemental) interpolation functions which have the following properties

$$\psi_\alpha(X^\beta) = \delta_\alpha{}^\beta, \qquad \sum_{\alpha=1}^{2} \psi_\alpha = 1.$$

In general, these local interpolation functions contain complete polynomials of degree p, where $p+1$ is the order of the highest material derivative that appears in the energy equation for the element. In this case, we have $p = 1$ (see [12]). Therefore, the particular elemental field quantity $f(X,t)$ is simply a linear function of the local coordinates of the elements; i.e.

$$f(X,t) \doteq \psi_\alpha(X)f_\alpha(t) = (a_\alpha + b_\alpha X)f_\alpha(t) \tag{4.4}$$

where, for any element

$$a_\alpha \sim [a_1, a_2] = [1, 0], \qquad b_\alpha \sim [b_1, b_2] = \frac{1}{h}[-1, 1]. \tag{4.5}$$

4.1 *Galerkin models for nonlinear wave propagation*

Using the local approximation (4.3) we can construct finite element models for (3.1) and (3.3) using the concept of weak or variational solutions. This naturally results in Galerkin-type models. Initially, consider (3.1), we seek weaker solutions to (3.1) by only requiring that

$$\int_0^h (\ddot{u} - c^2 u_{xx})\beta \, dX = 0 \tag{4.6}$$

for any arbitrary function $\beta(X)$ which has a continuous derivative and vanishes outside the

element. Similarly, we can seek weaker solutions of (3.3) by requiring that

$$\int_0^h (\ddot{\lambda} - (c^2\lambda_x)_x)\phi \, dX = 0 \tag{4.7}$$

where $\phi(X)$ is an arbitrary function which has a continuous first derivative and which vanishes outside the element.

There is an interesting relationship between (4.6) and (4.7). Integrating by parts and setting $\beta = -\partial\phi/\partial X$

$$\begin{aligned}\int_0^h (\ddot{\lambda} - (c^2\lambda_x)_x)\phi \, dX &= \int_0^h \frac{\partial}{\partial X}(\ddot{u} - c^2 u_{xx})\phi \, dX \\ &= -\int_0^h (\ddot{u} - c^2 u_{xx})\frac{\partial\phi}{\partial X} dX \\ &= \int_0^h (\ddot{u} - c^2 u_{xx})\beta \, dX. \end{aligned} \tag{4.8}$$

This result essentially implies that if λ satisfies (4.7), $\lambda = 1 + (\partial u/\partial X)$, and $\beta = -\partial\phi/\partial X$, then u satisfies (4.6). The converse also holds.

In our later work, we want to examine properties of the finite element models developed from (4.6) and (4.7) using certain fundamental ideas of finite elements concerned with energy. Clearly, under certain conditions, finite element models developed from (4.6) and (4.7) are equivalent.

Now finite element models can be developed from (4.7) through the following procedure: Integrating (4.7) by parts gives

$$\int_0^h \ddot{\lambda}\phi \, dX + \int_0^h \frac{1}{\rho_0}\frac{\partial\sigma}{\partial X}\phi_x \, dX = \left[\frac{1}{\rho_0}\frac{\partial\sigma}{\partial X}\phi\right]_0^h \tag{4.9}$$

where, from (3.2), $\partial\sigma/\partial X = (\partial\alpha/\partial\lambda)\lambda_x = c^2\lambda_x$. If ϕ_x is constant, (4.9) becomes

$$\int_0^h \ddot{\lambda}\phi \, dX + \frac{1}{\rho_0}\phi_x[\sigma]_0^h = [c^2\lambda_x\phi]_0^h. \tag{4.10}$$

Taking a piecewise linear approximation (4.3) for λ, we have

$$\lambda(X, t) = \psi_\alpha(X)\lambda_\alpha(t) = (a_\alpha + b_\alpha X)\lambda_\alpha \tag{4.11}$$

where a_α and b_α are defined in (4.5). Hence, with (4.5) in (4.11), we have

$$\begin{aligned}\lambda_x &= \psi_{\alpha,x}\lambda_\alpha = b_\alpha\lambda_\alpha = \frac{1}{h}(\lambda_2 - \lambda_1) \\ \psi_{\alpha,x} &= b_\alpha = \frac{1}{h}[-1, 1]. \end{aligned} \tag{4.12}$$

Taking $\phi(X) = \psi_\alpha(X)$ in (4.10) and incorporating (4.12), we obtain the equation of motion for a typical rod element

$$m_{\beta\alpha}\ddot{\lambda}_\beta + b_\alpha A_0[\sigma]_0^h = p_\alpha \tag{4.13}$$

where $m_{\beta\alpha}$ is the consistent mass matrix defined by

$$m_{\beta\alpha} = m_{\alpha\beta} = \rho_0 A_0 \int_0^h \psi_\beta \psi_\alpha \, dX \tag{4.14}$$

p_α is the generalized force at node α

$$p_\alpha = \rho_0 A_0[\psi_\alpha c^2 \lambda_x]_0^h. \tag{4.15}$$

Equation (4.14) can be integrated to get the consistent mass matrix in the form

$$m_{\beta\alpha} = \tfrac{1}{6} m(1 + \delta_{\beta\alpha}) \tag{4.16}$$

where $m = \rho_0 A_0 h$ is the mass of a typical element and $\delta_{\beta\alpha}$ is the Kronecker delta. However, if the mass is considered to be lumped at the nodes, $m_{\beta\alpha}$ will be of the diagonal form, $m\delta_{\beta\alpha}/2$. We prefer the lumped mass model in this study, not only for the increased computational speed, but also because it tends to maintain the finite character of the speed at which waves are propagated along the rod while simultaneously reducing "ringing" in front of the wave front.

We now turn to the displacement form of the equation of motion (3.1). We develop finite element models from (4.6) using the same procedure used for (4.8); that is, we approximate the local displacement field by

$$u(X, t) = \psi_\alpha(X) u_\alpha(t) = (a_\alpha + b_\alpha X) u_\alpha \tag{4.17}$$

with a_α and b_α defined in (4.5), and here $u_\alpha = u(X_\alpha, t)$. Accordingly, taking $\beta(X) = \psi_\alpha(X)$ in (4.6), we obtain as the equation of motion for a typical rod element,

$$m_{\beta\alpha}\ddot{u}_\beta + b_\alpha A_0 h\sigma = p_\alpha.$$

In this case, since $u_x = b_\alpha u_\alpha$, both λ and $\sigma = \sigma(\lambda)$ are constant for each element. The mass matrix is as previously defined, but the generalized nodal force p_α is now

$$p_\alpha = A_0 \sigma[\psi_\alpha]_0^h. \tag{4.18}$$

4.2 *Global form of the equations of motion*

To facilitate book-keeping, we use superscripts as the element index and subscripts as the nodal index. If we define P_N as the net generalized force applied at node N, so that $P_N = p_2^{N-1} + p_1^N$, then the global equation of motion for node N is obtained from (4.13) as

$$P_N = m\ddot{\lambda}_N - \frac{A_0}{h}(\sigma_{N-1} - 2\sigma_N + \sigma_{N+1}) \tag{4.19}$$

where, from (4.5), $b_N^{N-1} = +h^{-1}$ and $b_N^N = -h^{-1}$, and we have used the lumped mass model. At the ends of the rod, of course, the form of (4.19) changes according to the type of boundary conditions. Equations (4.19) represent the global system of nodal equations of motion for the

finite-element model of the rod. Since the solution to these equations will be in terms of the displacement gradients ($\lambda - 1 = \partial u/\partial x$), the nodal displacements, if desired, are obtained by spatial integration.

The displacements can be obtained directly if the global equations of motion are formed as above, but using (4.18) rather than (4.13):

$$P_N = m\ddot{u}_N + A_0(\sigma^{N-1} - \sigma^N). \tag{4.20}$$

4.3 *Justification of the finite element method for the analysis of wave propagation problems*

In order to justify the finite element models of shock smearing type introduced in Section 4.1, we show that in the neighborhood of surfaces of discontinuity, such as shock waves in hyperelastic bodies, the jump conditions are satisfied in an average sense.

In equation (4.17) we introduced the finite element approximation for the local displacement field. In this section we would like to introduce a more general displacement approximation. This displacement approximation would allow jumps in the first spatial and temporal derivatives as long as they are compatible with the kinematic compatibility equation (2.15). We use the same notation for the displacement approximation as was introduced in (4.17)

$$u = u_\alpha \psi_\alpha. \tag{4.21}$$

However, we intend that the parameters u_α represent the nodal displacements in the element plus certain generalized coordinates which involve the shock strength and shock position and are continuously differentiable functions of time. In this case the trial functions $\psi_\alpha(X)$ must be chosen from a very general class of functions. This class is made up of the union of class $C(0, h)$ of those functions which are continuous everywhere in the element and the class $J(0, h)$ of functions which have a finite jump at the surface of discontinuity S but are continuous everywhere else in the element.

The finite-element representation for the local material velocity and acceleration can be obtained by differentiating (4.21):

$$\dot{u}(X, t) = \dot{u}_\alpha(t)\psi_\alpha(X)$$
$$\ddot{u}(X, t) = \ddot{u}_\alpha(t)\psi(X).$$

From (4.21) we can see that if the trial functions are continuous everywhere, the first temporal derivative must be a continuous function of X, and a shock smearing scheme would result. However, if the trial functions were discontinuous, shock fitting schemes would be obtained.

Consider the typical element containing a surface of discontinuity S as shown in Fig. 4. The global energy balance for this finite element is of the form

$$A_0 \int_{h-Y} (\rho_0 \dot{u}\ddot{u} - \sigma_x \dot{u})\, \mathrm{d}X + \frac{1}{2}\rho_0 A_0 c[\![\dot{u}^2]\!]_Y + A_0[\![\sigma\dot{u}]\!]_Y - A_0\bar{\sigma}[\![\dot{u}]\!]_Y = 0 \tag{4.22}$$

where we have used (2.5), assumed the local energy relations $(2.8)_2$ and (2.12) are identically satisfied, and eliminated the internal energy terms. Now, the second term of the integral in (4.22) can be integrated by parts

$$A_0 \int_{h-Y} \sigma_x \dot{u}\, \mathrm{d}X = -A_0 \int_{h-Y} \sigma\dot{u}_x\, \mathrm{d}X + A_0[\sigma\dot{u}]_0^h + A_0[\![\sigma\dot{u}]\!]_Y \tag{4.23}$$

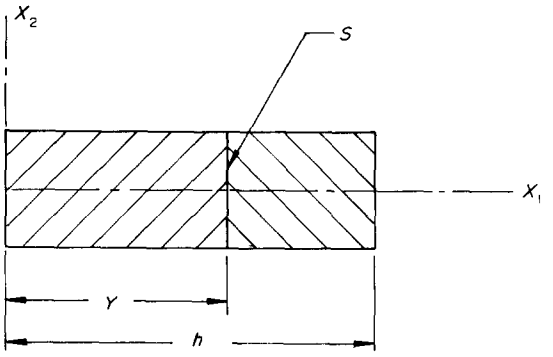

Fig. 4.

so that, with (4.23), (4.22) can be rewritten as

$$A_0 \int_{h-Y} (\rho_0 \dot{u}\ddot{u} - \sigma \dot{u}_x)\, \mathrm{d}X - A_0[\sigma \dot{u}]_0^h + \frac{1}{2}\rho_0 A_0 c[\![\dot{u}^2]\!]_Y - A_0 \bar{\sigma}[\![\dot{u}]\!]_Y = 0. \tag{4.24}$$

Introducing the local finite element approximation (4.17) for the displacement u and its derivatives in (4.24), we have

$$\left\{A_0 \int_{h-Y} (\rho_0 \psi_\alpha \psi_\beta \ddot{u}_\beta + \sigma \psi_{\alpha,x})\, \mathrm{d}X - A_0[\sigma \psi_\alpha]_0^h + \frac{1}{2}\rho_0 A_0 c[\![\psi_\alpha \psi_\beta]\!]_Y \dot{u}_\beta - A_0 \bar{\sigma}[\![\psi_\alpha]\!]_Y\right\}\dot{u}_\alpha = 0$$

where, at this point, we need not specify the precise form of the local interpolation functions $\psi_\alpha(X)$. The above equation can be written more compactly as

$$\left(M_{\alpha\beta}\ddot{u}_\beta + A_0 \int_{h-Y} \sigma \psi_{\alpha,x}\, \mathrm{d}X - P_\alpha + R_{\alpha\beta}\dot{u}_\beta - S_\alpha\right)\dot{u}_\alpha = 0 \tag{4.25}$$

where we have defined

$$\begin{aligned} M_{\alpha\beta} &= \rho_0 A_0 \int_{h-Y} \psi_\alpha \psi_\beta\, \mathrm{d}X \\ P_\alpha &= A_0[\sigma \psi_\alpha]_0^h \\ R_{\alpha\beta} &= \frac{1}{2}\rho_0 A_0 c[\![\psi_\alpha \psi_\beta]\!]_Y \\ S_\alpha &= A_0 \bar{\sigma}[\![\psi_\alpha]\!]_Y. \end{aligned} \tag{4.26}$$

Since (4.25) must be valid for arbitrary motions of the element, it must also hold for arbitrary values of the nodal velocities $\dot{u}_\alpha$. In particular, if (4.25) is to hold for arbitrary $\dot{u}_\alpha$, the term in the parentheses must vanish for all values of α. Thus,

$$M_{\alpha\beta}\ddot{u}_\beta + A_0 \int_{h-Y} \sigma \psi_{\alpha,x}\, \mathrm{d}X - P_\alpha + R_{\alpha\beta}\dot{u}_\beta - S_\alpha = 0. \tag{4.27}$$

This equation represents the consistent finite-element equations of motion with shock terms. Thus, as might be expected, a consistent finite element momentum equation for nonlinear wave propagation problems contains the proper jump conditions at the shock.

Based on the above development, we now examine the finite element model (4.18) developed from (4.6) and the model (4.13) developed from (4.7). We will show that (4.13) and (4.18) can be obtained from global balance laws, that using global energy balances and the modeling procedure introduced above insures that the jump conditions (2.9) are satisfied in an average sense, and that this implies that (4.13) and (4.18) satisfy the jump conditions in an average sense.

If the functions $\psi_\alpha(X)$ in (4.27) are assumed to be continuous, then $R_{\alpha\beta} = S_\beta = 0$ $(\alpha, \beta = 1, 2)$. We examine two cases. First, if the $\psi_\alpha(X)$ are linear over the element, the finite element scheme (4.18) is obtained. Thus the finite element model (4.18) can be derived from the global energy balance (2.5). Secondly, suppose the $\psi_\alpha(X)$ are constant over the element and the $\phi(X)$ introduced in (4.7) are related to the $\psi_\alpha(X)$ by taking $\phi(X) = \xi_\alpha(X)$ and

$$\psi_\alpha(X) = \frac{\partial \xi_\alpha(X)}{\partial X}.$$

Then the $\xi_\alpha(X)$ are linear functions. This implies that models of the form (4.13) can be derived from energy principles. To see this, simply set $\phi = \xi_\alpha(X)$ and $\beta = -\psi_\alpha(X)$ in (4.8). Thus both models of the form (4.13) and (4.18) can be derived from energy balances of the form (2.5) if certain restrictions are placed on the trial functions.

4.4 *Satisfaction of jump conditions*

Now the important question that arises is whether or not the jump conditions (2.9) are satisfied in an average sense in the element when the global energy balances described are used to derive finite element models. In this discussion, by "an average sense" we mean in a sense at least as weak as $L_1(0, h)$. This is certainly true of $(2.9)_2$ since it was obtained from a global energy balance (2.5) by shrinking the volume of the rod to zero at the surface of discontinuity while holding A_0 constant. In addition, in our derivation, we assumed that (2.12) was identically satisfied on the surface of discontinuity S. Now if (2.12) is satisfied exactly while $(2.9)_2$ is satisfied in an average sense, then $(2.9)_1$ is satisfied in a average sense (see the derivation of (2.12)). In addition, the Clausius–Duhem inequality $(2.9)_3$ is satisfied because of the constitutive assumptions introduced in section 2.3. Thus, the use of the global energy balance (2.5) and the procedure introduced above insures that the local jump conditions (2.9) are satisfied in an average sense across the element if the element is sufficiently small. To complete the argument, we conclude that because (4.13) and (4.18) can be derived from global energy balances they satisfy the local jump conditions in an average sense in the element.

5. FINITE ELEMENT/DIFFERENCE EQUATIONS

The remaining step in discretizing the nonlinear equations is approximating their temporal behavior. Solving the nonlinear equations of motion by stepwise numerical methods can be severely complicated by the presence of shocks. Therefore, we choose an explicit finite difference scheme which automatically treats the shocks, whenever and wherever they may occur, without necessity of the tedious application of the jump conditions at each time step of the solution process. This method is the well-known Lax–Wendroff difference scheme [27, 28], which is generally classified as an artificial dissipative method. The success of this particular method comes from applying finite difference approximations to the governing equations expressed as

"conservation" laws. (For details of the theory of conservation laws and weak solutions (see, e.g. [23, 27, or 29]). The novel aspect of the following temporal discretization is that, by rewriting (3.1) as (3.3) we obtain the governing equation in the form of a conservation law which, with only a linear finite-element approximation, enables us to develop a Lax–Wendroff type integration scheme.

5.1 *Lax–Wendroff finite-element scheme*

The temporal discretization is accomplished in the spirit of the Lax–Wendroff equations (see [28], p. 302): we first denote $\dot{q}_N = \ddot{\lambda}_N$ and expand $q_N(t+\Delta t)$ into a Taylor series up to second order terms

$$q_N(t+\Delta t) = q_N(t) + \Delta t \dot{q}_N + \tfrac{1}{2}(\Delta t)^2 \ddot{q}_N + 0(\Delta t^3). \tag{5.1}$$

The t derivatives in (5.1) are now replaced by X derivatives (except for the nodal force P_N) by means of (4.17) where

$$\dot{q}_N = \frac{A_0}{mh}(\sigma_{N-1} - 2\sigma_N + \sigma_{N+1}) + \frac{1}{m} P_N \tag{5.2}$$

$$\ddot{q}_N = \frac{\partial}{\partial t}\dot{q}_N = \frac{A_0}{mh}(\dot{\sigma}_{N-1} - 2\dot{\sigma}_N + \dot{\sigma}_{N+1}) + \frac{1}{m}\dot{P}_N. \tag{5.3}$$

Since $\sigma = \sigma(\lambda)$, $\dot{\sigma} = \rho_0 c^2 q$, so that (5.3) becomes

$$\ddot{q}_N = \frac{1}{h^2}(c^2_{N-1} q_{N-1} - 2c_N{}^2 q_N + c^2_{N+1} q_{N+1}) + \frac{1}{m}\dot{P}_N. \tag{5.4}$$

Note that since the quantities P_N are prescribed, so also are the $\dot{P}_N$ (e.g. if $P_N = \sin t$, then $\dot{P}_N = \cos t$). Substituting (5.2) and (5.4) into (5.1), we obtain the finite element/difference equation for the interior nodes of the discrete model:

$$\begin{aligned} q_N{}^{n+1} = {} & \left(\frac{\Delta t}{h}\right)^2 \left[\frac{1}{2}(c^n_{N+1})^2 q^n_{N+1} + \left\{\left(\frac{h}{\Delta t}\right)^2 - (c_N{}^n)^2\right\} q_N{}^n + \frac{1}{2}(c^n_{N-1})^2 q^n_{N-1}\right] \\ & + \frac{\Delta t A_0}{mh}(\sigma^n_{N-1} - 2\sigma_N{}^n + \sigma^n_{N+1}) + \frac{1}{2m}[2\Delta t P_N{}^n + (\Delta t)^2 \dot{P}_N{}^n] \end{aligned} \tag{5.5}$$

where $t = n\Delta t$, and $q(t) = q(n\Delta t) = q^n$, etc. Similarly, the finite element/difference equations for the end nodes are

$$q_1{}^{n+1} = \left(\frac{\Delta t}{h}\right)^2 \left[(c_2{}^n)^2 q_2{}^n + \left\{\left(\frac{h}{\Delta t}\right)^2 - (c_1{}^n)^2\right\} q_1{}^n\right] + 2\frac{\Delta t A_0}{mh}(\sigma_2{}^n - \sigma_1{}^n) + \frac{1}{m}[2\Delta t P_1{}^n + (\Delta t)^2 \dot{P}_1{}^n] \tag{5.6}$$

and

$$\begin{aligned} q^{n+1}_{E+1} = {} & \left(\frac{\Delta t}{h}\right)^2 \left[(c_E{}^n)^2 q_E{}^n + \left\{\left(\frac{h}{\Delta t}\right)^2 - (c^n_{E+1})^2\right\} q^n_{E+1}\right] + 2\frac{\Delta t A_0}{mh}(\sigma_E{}^n - \sigma^n_{E+1}) \\ & + \frac{1}{m}[2\Delta t P^n_{E+1} + (\Delta t)^2 \dot{P}^n_{E+1}]. \end{aligned} \tag{5.7}$$

To compute the extension ratios, we simply repeat the foregoing procedure: we first expand $\lambda_N{}^{n+1}$:

$$\lambda_N{}^{n+1} = \lambda_N{}^n + \Delta t q_N{}^n + \left(\frac{\Delta t}{2}\right)^2 \dot{q}_N{}^n + 0(\Delta t^3) \tag{5.8}$$

and so, using (5.2), we get:

$$\begin{aligned}
\lambda_N{}^{n+1} &= \lambda_N{}^n + \Delta t q_N{}^n + \frac{1}{2\rho_0}\left(\frac{\Delta t}{h}\right)^2 (\sigma^n_{N-1} - 2\sigma_N{}^n + \sigma^n_{N+1}) + \frac{(\Delta t)^2}{2m} P_N{}^n \\
\lambda_1{}^{n+1} &= \lambda_1{}^n + \Delta t q_1{}^n + \frac{1}{\rho_0}\left(\frac{\Delta t}{h}\right)^2 (\sigma_2{}^n - \sigma_1{}^n) + \frac{(\Delta t)^2}{m} P_1{}^n \\
\lambda^{n+1}_{E+1} &= \lambda^n_{E+1} + \Delta t q^n_{E+1} + \frac{1}{\rho_0}\left(\frac{\Delta t}{h}\right)^2 (\sigma_E{}^n - \sigma^n_{E+1}) + \frac{(\Delta t)^2}{m} P^n_{E+1}
\end{aligned} \tag{5.9}$$

where $\sigma_N{}^n$ and $(c_N{}^n)^2$ are determined from (3.4) and (3.2) respectively.

Equations (5.5)–(5.7) and (5.9) are the $2(E+1)$ finite element/difference equations used herein for the study of shock waves.

5.2 *Velocity formulated central difference scheme*

To illustrate the effectiveness of the Lax–Wendroff method we will compare the results with the finite element/difference equations which are obtained using the displacement equations (4.18). The temporal discretization is accomplished for these equations by using velocity formulated central differences[30], in which the general nodal equation, $\ddot{u}_N(t) = F(t)$, is approximated by introducing the nodal velocity $v_N = \dot{u}_N$ and thereby generating two equivalent first order equations, which are then differenced to obtain

$$\begin{aligned}
v_N{}^{n+1/2} &= v_N{}^{n-1/2} + \Delta t F_N{}^n \\
u_N{}^{n+1} &= u_N{}^n + \Delta t v_N{}^{n+1/2}.
\end{aligned} \tag{5.10}$$

Direct substitution shows that (5.10) is equivalent to using the usual central difference approximation for $\ddot{u}_N$. However (5.10) generally admits to less round-off error (see [30]).

6. NUMERICAL RESULTS

In this section, we cite numerical results obtained from application of the preceding theory to representative problems. For our numerical examples, we consider a thin rod of Mooney material ($C_1 = 24{\cdot}0$ psi, $C_2 = 1{\cdot}5$ psi) with the following undeformed characteristics: length = 3·0 inches, cross-sectional area = 0·0314 in^2, mass density = 10^{-4} lb.sec^2/in^4. For the finite element model, we take 60 evenly spaced elements, so that $h = 0{\cdot}05$ in. and $E = 60$.

6.1 *Tensile loading (square wave)*

We consider a force of constant magnitude applied at the free end of the rod as a step function at $t = 0$, then similarly removed at a later time $t = t^*$, i.e. a square wave. For this example, $t^* = 0{\cdot}002$ seconds. Figure 5 shows the stress wave response to a two pound step loading (this corresponds to 86% strain statically) for both mass distributions and both time integration

schemes previously discussed. Several important items mentioned earlier can be observed in Fig. 5.

(1) The lumped mass model tends to preserve the finiteness of the speed of propagation. (Note the "ringing" in front of the consistent mass stress wave.)

(2) The acceleration wave front does tend to flatten with time.

(3) The wave is propagated into the undisturbed portion of the rod as a simple wave. Recall that for a simple wave, $Y(t)$ is constant, so that by multiplying $Y(0{\cdot}001)$ by 2·0—the ratio of the elapsed time increments—we obtain $Y(0{\cdot}002)$, except, of course, for that portion of the wave affected by the fixed boundary.

(4) The Lax–Wendroff scheme appears to be effective for short time periods, particularly in the presence of shocks. Not only does it produce no ringing in front of the wave, but the unloading shock wave is depicted without the large oscillations behind the shock. (These oscillations have been interpreted by some as numerical instability of the integration scheme. This is not so; the amplitude of these oscillations does not change with time. As pointed out in [28], these are lumped mass oscillations resulting from discretization error and they represent the internal energy which must appear in the "shocked" region according to the jump conditions. It appears that the Lax–Wendroff scheme has sufficient dissipation to convert this oscillatory energy into a good approximation of the internal energy.)

Figure 6 shows in some detail the response of the rod to this 2-lb step load. The results confirm the fact that weak shocks propagate in a manner similar to simple waves—the stress increases at the wall almost by a factor of 2·0 and the stress wave is reflected from the wall without appreciable change in shape or magnitude.

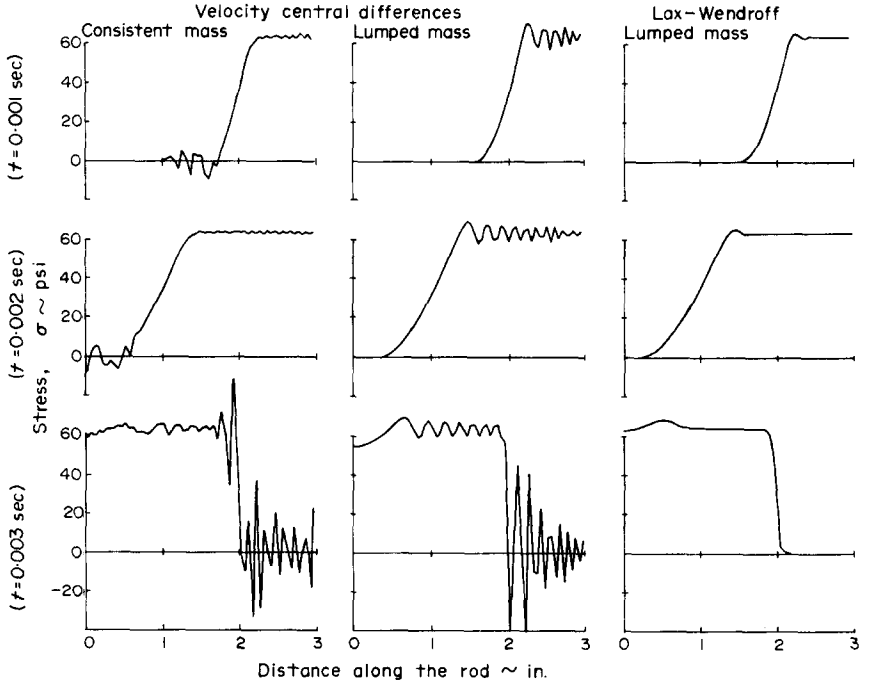

Fig. 5.

6.2 *Sinusoidal forcing function*

This example dramatically illustrates that the central difference scheme, without modification, cannot handle shocks. Here a concentrated, time-dependent load which varies sinusoidally is applied at the free end; a complete loading cycle occurs in 0·002 seconds. It is clear from the computed response shown in Fig. 7 that shocks develop quickly for this kind of loading. Unlike the response for the tensile step load where the unloading wave is produced by simply removing the load, the sinusoidal load actually "pushes" the end of the rod. The instant the load starts to decrease is the moment when the first wavelet is generated which propagates faster than the

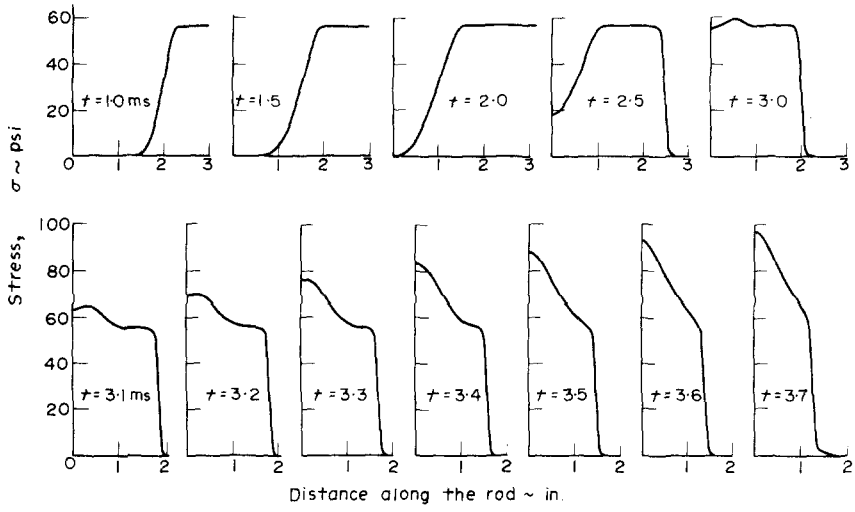

Fig. 6(a).

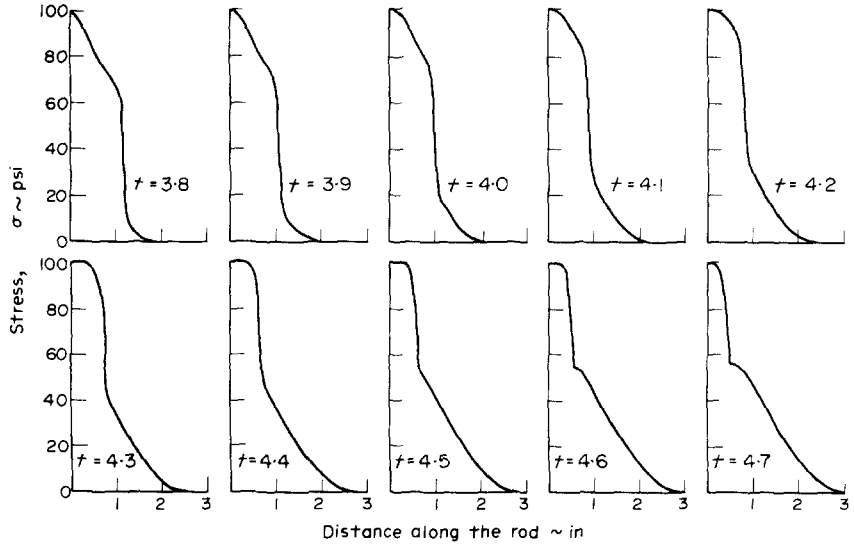

Fig. 6(b).

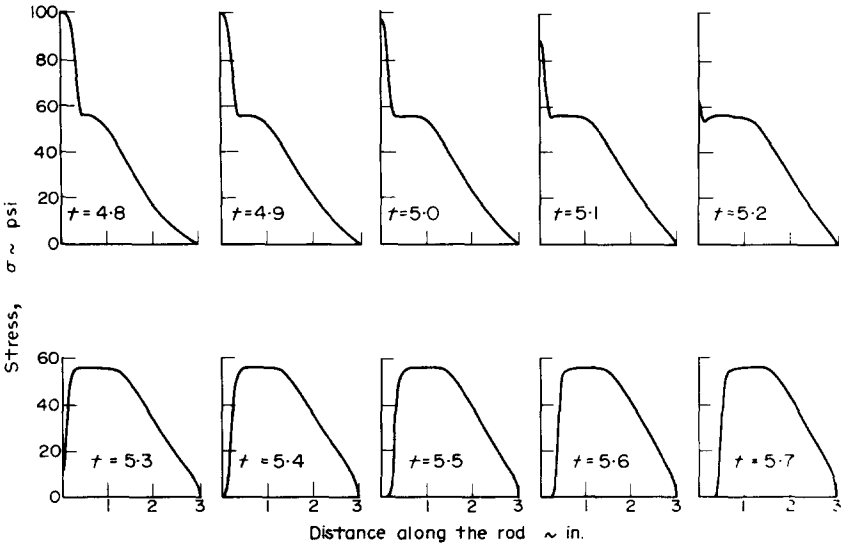
Stress, σ ~ psi
100
80
60
40
20
0
t = 4·8
t = 4·9
t = 5·0
t = 5·1
t = 5·2
60
40
20
0
t = 5·3
t = 5·4
t = 5·5
t = 5·6
t = 5·7
1
2
3
Distance along the rod ~ in.

Fig. 6(c).

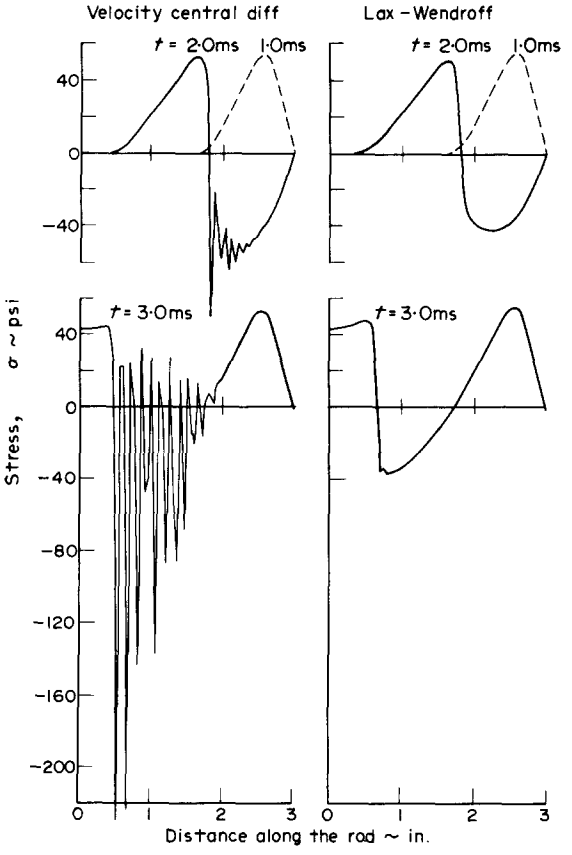
Velocity central diff
Lax – Wendroff
t = 2·0ms
1·0ms
40
0
-40
t = 3·0ms
Stress, σ ~ psi
40
0
-40
-80
-120
-160
-200
0
1
2
3
Distance along the rod ~ in.

Fig. 7.

preceding one. Thus, at some time subsequent to when the compression cycle starts, a compression shock forms in the rod.

A comparison between the two integration schemes is also shown in Fig. 7 for the sinusoidal loading. In this case, it is clear that the "shocked internal energy" behind the compression shock renders the central difference scheme unacceptable. It is interesting to note, however, that the tension cycle evidently "absorbs" the large oscillations preceding it and again produces a smooth

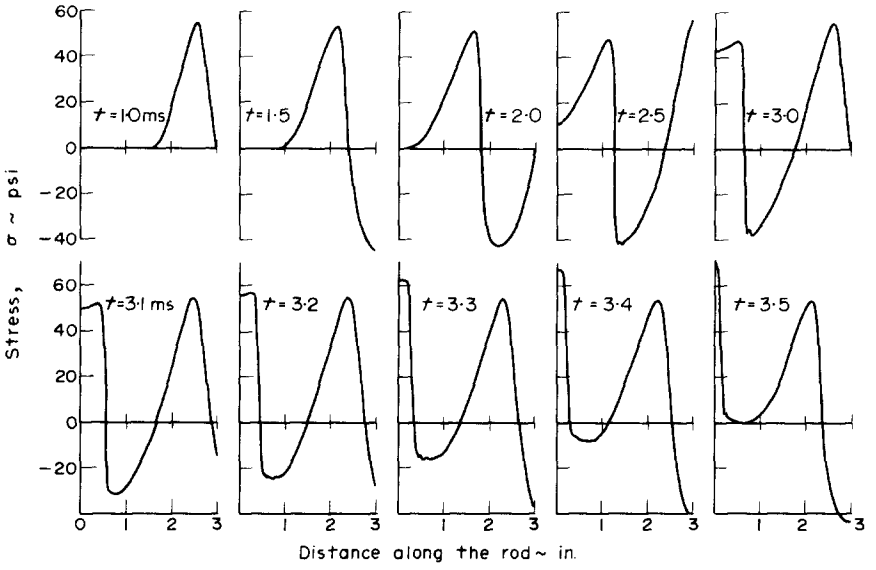

Fig. 8(a).

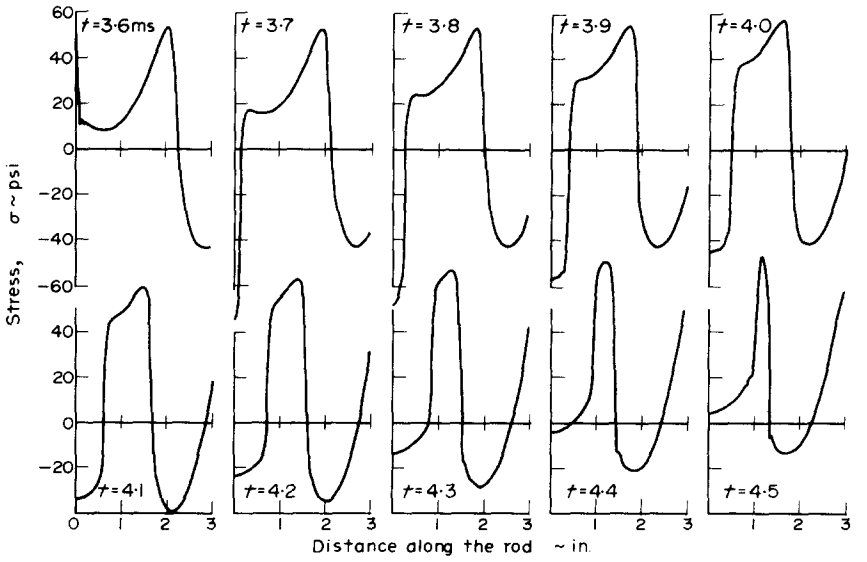

Fig. 8(b).

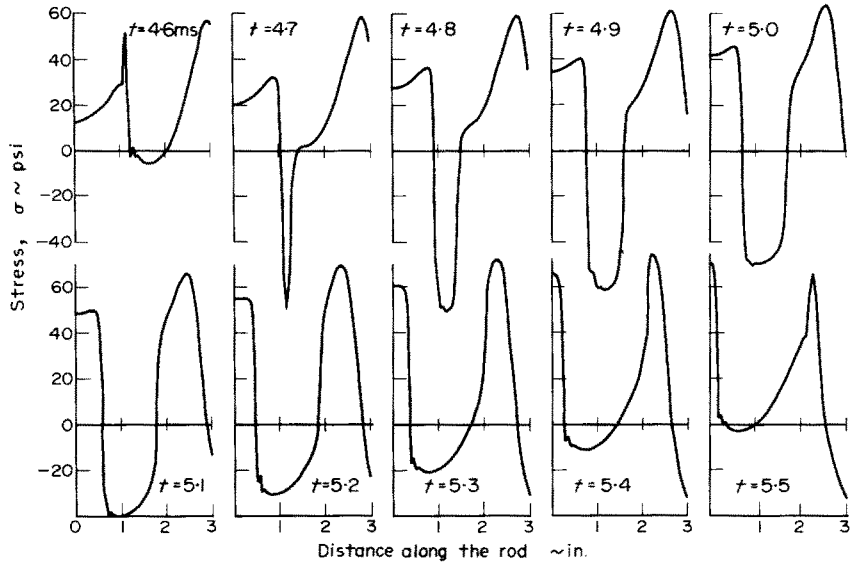
t=4·6ms
t=4·7
t=4·8
t=4·9
t=5·0
t=5·1
t=5·2
t=5·3
t=5·4
t=5·5
Stress, σ ~ psi
Distance along the rod ~in.

Fig. 8(c).

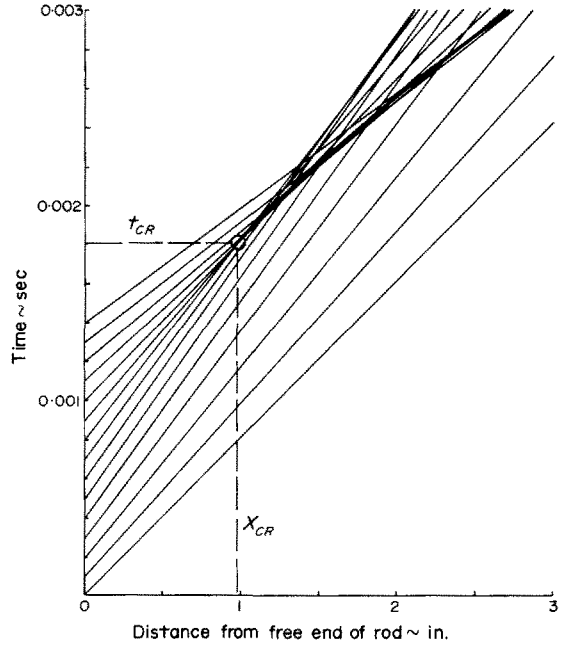
0·003
0·002
0·001
t_{CR}
X_{CR}
Time ~ sec
Distance from free end of rod ~ in.

Fig. 9.

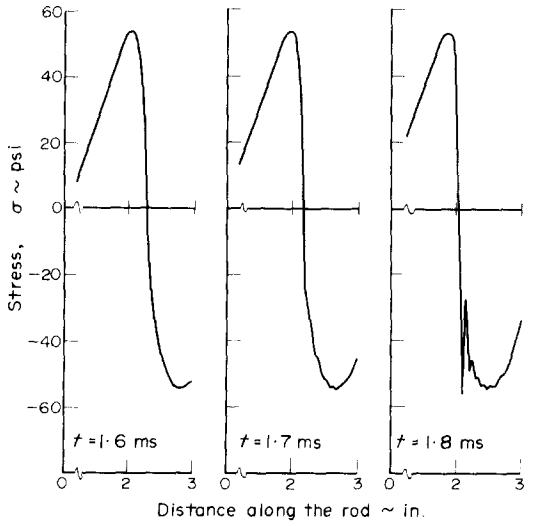

Fig. 10.

wave front. The detailed response to this loading is shown in Fig. 8. From the response shown, we notice several interesting features of nonlinear wave motion:

The compressive shock wave is reflected from the wall as a compressive shock wave by almost doubling the compressive stress; but the tension part of the stress wave is reflected with only a small increase in stress.

At $t = 4{\cdot}7$ millisec, two compression shocks collide. The numerical results shown here indicate that when two shocks collide in a solid material, they penetrate one another with little or no deterioration. This is apparently contrary to the collision of shocks in gases[21].

By comparing the response at $t = 3$ msec with that at $t = 5$ msec, we note that the response tends to repeat itself (with some variation due to the reflection) with essentially the same period as that of the forcing function.

As in the development of shocks from Lipschitz continuous data, the shock forms subsequent to initiation of the compressive cycle. Thus we are led to examine the positive slope characteristics in the X–t plane to see if they predict t_{CR} for this type of loading. Figures 9 and 10 show that if we assume straight compression characteristics of positive slope, the cusp of the corresponding envelope in the X–t plane does, in fact, give a good estimate of the t_{CR} observed in the stress–time plots.

Acknowledgements—This work was completed at The University of Texas at Austin under the support of the National Science Foundation through grant GK-39071. Phases of the work were done at the Research Institute of the University of Alabama in Huntsville through support of the U.S. Air Force Office of Scientific Research under Contract F44620-69-0124.

REFERENCES

1. C. A. Truesdell, The Mechanical Foundations of Elasticity and Fluid Dynamics, *J. Rational Mechanics and Analysis* **1**, 125–300 (1952).
2. R. S. Rivlin, Large Elastic Deformations of Isotropic Materials. I. Fundamental Concepts, *Phil. Trans. Royal Society of London*, **A240**, 459–490 (1948).
3. J. K. Knowles, Large Amplitude Oscillations of a Tube of Imcompressible Elastic Material, *Quart. appl. Maths.* **18**, 71 (1960).
4. J. K. Knowles, On a Class of Oscillations in the Finite-Deformation Theory of Elasticity, *J. Appl. Mech.* **29**, 283 (1962).

5. J. K. Knowles and M. T. Jakub, Finite Dynamic Deformation of an Incompressible Elastic Medium Containing a Spherical Cavity, *Archive for Rational Mechanics and Analysis* **14**, 367 (1965).
6. C. A. Truesdell and R. Toupin, The Classical Field Theories, in *Encyclopedia of Physics*, Vol. III/1. Springer, New York (1960).
7. H. Kolsky, *Stress Waves in Solids*. Clarendon Press, Oxford (1953); Dover Reprint (1964).
8. D. R. Bland, *Nonlinear Dynamic Elasticity*. Blaisdell, Waltham, Mass. (1969).
9. B. T. Chu, Finite Amplitude Waves in Incompressible Perfectly Elastic Materials, *J. Mech. Phys. Solids* **13**, 17–28 (1965).
10. J. T. Oden and J. Poe, On the Numerical Solution of a Class of Problems in Dynamic Coupled Thermoelasticity, *Developments in Theoretical and Applied Mechanics*, Vol. V, Proceedings of the Fifth Southeastern Conference on Theoretical and Applied Mechanics (1970), Raleigh, North Carolina, Pergamon Press, Oxford.
11. J. T. Oden and W. H. Armstrong, Analysis of Nonlinear, Dynamic Coupled Thermoviscoelasticity Problems by the Finite Element Method, *Int. J. Computers and Struct.* **1**, 603–621 (1971).
12. J. T. Oden, *Finite Elements of Nonlinear Continua*. McGraw-Hill, New York (1972).
13. H. Kolsky, Production of Tensile Shock Waves in Stretched Natural Rubber, *Nature* **224** (No. 5226), 1301 (1969).
14. A. E. Green and W. Zerna, *Theoretical Elasticity*, Second Edition, Oxford University Press (1968).
15. A. E. Green and J. E. Adkins, *Large Elastic Deformations*, Second Edition, Oxford University Press (1970).
16. J. L. Nowinski, On the Propagation of Finite Disturbances in Bars of Rubberlike Materials, *J. Engng. for Industry, ASME* **87**, 523–529 (1965).
17. W. F. Ames, On Wave Propagation in One-Dimensional Rubberlike Materials, *J. of Mathematical Analysis and Applications* **34** (No. 1), 214–222 (1971).
18. D. P. Reddy and J. D. Achenbach, Simple Waves and Shock Waves in a Thin Prestressed Elastic Rod, *ZAMP* **19**, 473–485 (1968).
19. D. R. Bland, Dilatational Waves and Shocks in Large Displacement Isentropic Dynamic Elasticity, *J. Mech. Phys. Solids* **12**, 245–267 (1964).
20. W. D. Collins, One-Dimensional Non-Linear Wave Propagation in Incompressible Elastic Materials, *Quart. J. Mechanics and Appl. Maths.* **19**, 259–328 (1966).
21. R. Courant and K. O. Friedrichs, *Supersonic Flow and Shock Waves*. Interscience, New York (1948).
22. A. H. Shapiro, *The Dynamics and Thermodynamics of Compressible Fluid Flow*, Vol. 1. The Ronald Press Co., New York (1953).
23. R. Courant and D. Hilbert, *Methods of Mathematical Physics*, Vol. II. Interscience, New York (1962).
24. W. F. Ames, Discontinutiy Formation in Solids of Homogeneous Non-Linear Hyperbolic Equations Possessing Smooth Initial Data, *Int. J. Non-Linear Mechanics* **5**, 605–615 (1970).
25. P. D. Lax, Development of Singularities of Solutions of Non-Linear Hyperbolic Partial Differential Equations, *J. Math. Phys.* **5** (No. 5), 611–613, (1964).
26. A. Jeffrey, The Evolution of Discontinuities in Solutions of Homogeneous Nonlinear Hyperbolic Equations Having Smooth Initial Data, *J. Math. and Mechanics* **17** (No. 4), 331–352 (1967).
27. P. Lax and B. Wendroff, Systems of Conservation Laws, *Communications on Pure and Appl. Math.* **13**, 217–237 (1960).
28. R. D. Richtmyer and K. W. Morton, *Difference Methods for Initial-Value Problems*, Second edition, Interscience Tracts in Pure and Applied Mathematics, No. 4. Interscience, New York (1967).
29. A. Jeffrey and T. Taniuti, *Non-Linear Wave Propagation*. Academic Press, New York (1964).
30. S. W. Key and Z. E. Beisinger, The Transient Dynamic Analysis of Thin Shells by the Finite Element Method, *Proc. Third Conf. on Matrix Methods in Structural Mechanics*, Wright-Patterson Air Force Base, Ohio (October, 1971).